



**NAVAL
POSTGRADUATE
SCHOOL**

MONTEREY, CALIFORNIA

THESIS

**PROCESSING OF NITI REINFORCED ADAPTIVE
SOLDER FOR ELECTRONIC PACKAGING**

by

William L. Wright

March 2004

Thesis Advisor: Indranath Dutta

Approved for public release; distribution is unlimited

THIS PAGE INTENTIONALLY LEFT BLANK

REPORT DOCUMENTATION PAGE			Form Approved OMB No. 0704-0188	
Public reporting burden for this collection of information is estimated to average 1 hour per response, including the time for reviewing instruction, searching existing data sources, gathering and maintaining the data needed, and completing and reviewing the collection of information. Send comments regarding this burden estimate or any other aspect of this collection of information, including suggestions for reducing this burden, to Washington headquarters Services, Directorate for Information Operations and Reports, 1215 Jefferson Davis Highway, Suite 1204, Arlington, VA 22202-4302, and to the Office of Management and Budget, Paperwork Reduction Project (0704-0188) Washington DC 20503.				
1. AGENCY USE ONLY (Leave blank)		2. REPORT DATE March 2004	3. REPORT TYPE AND DATES COVERED Master's Thesis	
4. TITLE AND SUBTITLE: Processing of NiTi Reinforced Adaptive Solder for Electronic Packaging			5. FUNDING NUMBERS	
6. AUTHOR(S) William L Wright			8. PERFORMING ORGANIZATION REPORT NUMBER	
7. PERFORMING ORGANIZATION NAME(S) AND ADDRESS(ES) Naval Postgraduate School Monterey, CA 93943-5000			10. SPONSORING/MONITORING AGENCY REPORT NUMBER	
9. SPONSORING /MONITORING AGENCY NAME(S) AND ADDRESS(ES) N/A			11. SUPPLEMENTARY NOTES The views expressed in this thesis are those of the author and do not reflect the official policy or position of the Department of Defense or the U.S. Government.	
12a. DISTRIBUTION / AVAILABILITY STATEMENT Approved for public release; distribution is unlimited			12b. DISTRIBUTION CODE	
13. ABSTRACT (maximum 200 words) Solder joints provide both electrical and mechanical interconnections between a silicon chip and the packaging substrate in an electronic application. The thermomechanical cycling (TMC) in the solder due to the mismatch of the coefficient of thermal expansion (CTE) between the silicon chip and the substrate causes numerous reliability challenges. This situation is aggravated by the ongoing transition to lead-free solders worldwide, and the trend towards larger, hotter-running chips. Therefore, improved solder joints, with higher resistance to creep and low-cycle fatigue, are necessary for future generations of microelectronics. This study reports in the development a process to fabricate solder joints with a fine distribution of shape memory alloys (SMA) NiTi particulates. The microstructure and interface zone of the as-reflowed solder-SMA composite has been characterized.				
14. SUBJECT TERMS Shape Memory Alloy, Thermomechanical Cycling, Low-cycle Fatigue, Shape Memory Effect, Nickel Titanium Solder			15. NUMBER OF PAGES 65	
			16. PRICE CODE	
17. SECURITY CLASSIFICATION OF REPORT Unclassified	18. SECURITY CLASSIFICATION OF THIS PAGE Unclassified	19. SECURITY CLASSIFICATION OF ABSTRACT Unclassified	20. LIMITATION OF ABSTRACT UL	

THIS PAGE INTENTIONALLY LEFT BLANK

Approved for public release; distribution is unlimited

**PROCESSING OF NITI REINFORCED ADAPTIVE SOLDER FOR
ELECTRONIC PACKAGING**

William L. Wright
Lieutenant, United States Navy
B.S., Auburn University, 1997

Submitted in partial fulfillment of the
requirements for the degree of

MASTER OF SCIENCE IN MECHANICAL ENGINEERING

from the

**NAVAL POSTGRADUATE SCHOOL
March 2004**

Author: William L. Wright

Approved by: Indranath Dutta
Thesis Advisor

Anthony J. Healey
Chairman, Department of Mechanical and
Astronautical Engineering

THIS PAGE INTENTIONALLY LEFT BLANK

ABSTRACT

Solder joints provide both electrical and mechanical interconnections between a silicon chip and the packaging substrate in an electronic application. The thermomechanical cycling (TMC) in the solder due to the mismatch of the coefficient of thermal expansion (CTE) between the silicon chip and the substrate causes numerous reliability challenges. This situation is aggravated by the ongoing transition to lead-free solders worldwide, and the trend towards larger, hotter-running chips. Therefore, improved solder joints, with higher resistance to creep and low-cycle fatigue, are necessary for future generations of microelectronics. This study reports in the development a process to fabricate solder joints with a fine distribution of shape memory alloys (SMA) NiTi particulates. The microstructure and interface zone of the as-reflowed solder-SMA composite has been characterized.

THIS PAGE INTENTIONALLY LEFT BLANK

TABLE OF CONTENTS

I.	INTRODUCTION.....	1
II.	BACKGROUND.....	5
A.	SOLDERS IN ELECTRONICS.....	5
1.	Basics.....	5
2.	Thermomechanical Behavior.....	6
B.	LEAD FREE SOLDER.....	9
1.	Introduction.....	9
2.	Composite Alloys.....	10
C.	NICKEL TITANIUM.....	12
1.	Basics.....	13
2.	Martensite/Austenite Phase Characteristics.....	16
3.	Inter-Metallic Wettability.....	18
III.	EXPERIMENTAL PROCEDURE.....	21
A.	NICKEL TITANIUM SIZING.....	21
1.	Procedure.....	21
B.	IMPROVING WETTABILITY.....	24
1.	Procedure.....	24
C.	SOLDER FLUX.....	25
1.	Procedure.....	25
D.	SOLDER PASTE.....	27
1.	Procedure.....	27
E.	COMPOSITE PASTE.....	28
1.	Procedure.....	28
F.	PRODUCTION OF COMPOSITE SOLDER.....	29
1.	Procedure.....	29
IV.	RESULTS AND DISCUSSION.....	31
A.	MICROSTRUCTURES.....	31
B.	INTERFACIAL CHARACTERIZATION.....	38
V.	SUMMARY.....	43
	LIST OF REFERENCES.....	45
	INITIAL DISTRIBUTION LIST.....	49

THIS PAGE INTENTIONALLY LEFT BLANK

LIST OF FIGURES

Figure 1.	A cross-section of a printed circuit board (PCB) and adaptive solder.....	2
Figure 2.	Thermally induced stress that solders may undergo during normal operation [18].....	7
Figure 3.	C). Transformation from the austenite to the martensite phase and shape memory effect. The high-temperature austenitic structure undergoes twinning as the temperature is lowered. This twinned structure is called martensite. The martensitic structure is easily deformed by outer stress into a particular shape, and the crystal structure undergoes parallel registry. When heated, the deformed martensite resumes its austenitic form, and the macroscopic shape memory phenomenon is seen [36].	16
Figure 4.	Typical stress-strain curves at different temperature relative to the transformation showing (a) austenite, (b) martensite and pseudoelastic behavior [36].....	18
Figure 5.	Diagram of wetting angle [35].....	19
Figure 6.	Hydrogen embrittlement setup.....	22
Figure 7.	Graphs of particle size distribution for Dynalloy $A_s=45^\circ\text{C}$ wire of 1mm diameter after 2 and 4 hours of mortar and pestle grinding following hydrogenation.	23
Figure 8.	Developed NITI paste.....	25
Figure 9.	Flux Production Setup.....	26
Figure 10.	Composite solder balls of ~1mm diameter on an aluminum substrate following surface cleaning.....	30
Figure 11.	Optical microscopy image of the monolithic solder ball at (a) 1500 and (b) 3000X.....	31
Figure 12.	Microstructure of solder ball with NiTi injected into the melt, showing (a) overall ball and areas of interest, and (b-e) higher magnification pictures showing that most of the NiTi particles are segregated near the top surface.....	33
Figure 13.	Particulate segregation near surface of ball when injected with PPG.	35
Figure 14.	Overall microstructure of the reflowed composite ball produced using the final methodology using a combination of solder paste and NiTi paste (a), along with microstructures of several regions in the ball (b-e), showing a uniform distribution of ~20 volume percent NiTi particles in SnAgCu.....	37
Figure 15.	Resulting NiTi solder interfacial zone using 3000X optical microscopy.....	38
Figure 16.	Image and line scan of NiTi/solder interface.....	39
Figure 17.	SEM image and elemental X-ray maps illustrating (a) BSE image, and maps of (b) Nickel, (c) Titanium, (d) Silver and (e) Tin obtained from a region of the composite solder near the vicinity of a NiTi particle.	41

THIS PAGE INTENTIONALLY LEFT BLANK

LIST OF TABLES

Table 1.	CTE data for various components in Electronic packaging [19-21].	8
Table 2.	Thermal conductivity of various solders compositions [19-21].	9
Table 3.	Alloys with shape memory effect characteristics. . .	13
Table 4.	Properties of binary Ni-Ti alloys	14

THIS PAGE INTENTIONALLY LEFT BLANK

ACKNOWLEDGMENTS

I would like to sincerely thank Professor Indranath Dutta for his guidance and continued support during the evolution of this research project.

I also want to thank Deng Pan for all his help and support in the successful completion of this project.

I would also like to thank my wife and children, who patiently understood that all the nights and weekends spent at school were very important to my achieving this monumental goal.

THIS PAGE INTENTIONALLY LEFT BLANK

I. INTRODUCTION

In flip-chip (FC) and ball-grid array (BGA) interconnection schemes in microelectronic packages, arrays of tiny solder balls provide electrical and mechanical connections between silicon chip and an organic circuit board. A cross-sectional schematic of a typical printed circuit board (PCB) is shown in figure 1(a). Due to the large coefficient of thermal expansion (CTE) mismatch between silicon and the organic substrate, the solder balls are subjected to severe thermo-mechanical cycling (TMC) conditions as the chip is periodically powered on and off, potentially resulting in solder failure and destruction of the package. The periodic cycling results in TMC throughout the integrated component, subjecting even the connecting solder balls to extreme creep and low-cycle fatigue (LCF) conditions and over time certain failure.

The International Technology Roadmap for Semiconductors (ITRS) [1] projects that associated with the advancement of CMOS technology between 2001 and 2005, the maximum size of high-performance chips will increase from 20mm square to 25mm square, the power consumed will increase from 115 to 160W, and the peak temperature to which the chip may be subjected (due to Joule heating) will increase from 155 to 175°C. And during the same period, the maximum package pin-count (which correlates directly with the number of solder joints per chip and inversely with the solder joint size) will increase from 2007 to 3158. In practical terms, this will amount to increasingly extreme TMC conditions, for which current solder alloys are not suitable.

As the electronic devices grow in size, and the operating temperature of the package increases, solder joints in microelectronic packages will be placed under increasing thermo-mechanical loads (i.e., thermal and shear

strain). These extreme conditions will cause substantial creep and thermo-mechanical fatigue during service, and pose a serious reliability threat [2-5]. One way to achieve better solder life performance is by designing 'smart' or 'adaptive' solders, which reduce strain concentrations within joints, thereby improving the overall performance of the solder.

As shown in Figure 1, the concept of such a 'smart' solder is established by incorporating martensitic shape memory alloy (SMA) whiskers or particles into the solder. An ideal candidate SMA has similar yield strength as the solder so that at the beginning of the TMC, the martensitic SMA will deform with the solder under thermal induced shear stress. When the temperature is elevated above the austenitic transformation temperature (A_s), the SMA particles or whiskers will transform from martensite to austenite, which leads to a large increase of SMA stiffness, along with a reversal to the unstrained shape. Consequently, the SMA will reversely deform alleviating the strain concentration within the regions of interest within the solder ball, thus substantially improving the solder durability.

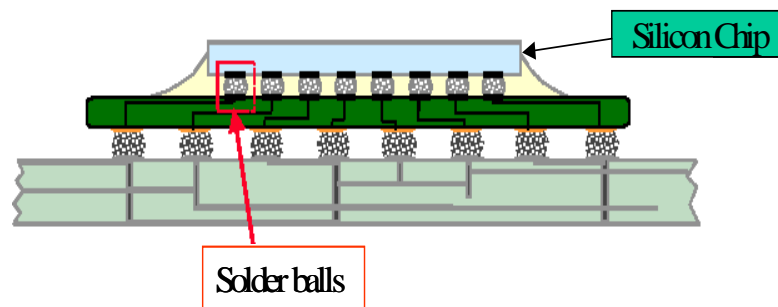


Figure 1. A cross-section of a printed circuit board (PCB) and adaptive solder.

However, to date, attempts to fabricate such 'smart solders have achieved a very limited success mainly due to the very poor wettability of SMA (e.g.NiTi) in the Sn containing matrix [6].

The objective of this thesis is to develop a fabrication process for a 'smart' or adaptive solder, wherein nickel titanium (NiTi) SMA particles are evenly distributed within a solder matrix, such that during TMC the SMA particles reduce the inelastic strain concentrations within the solder joints via internal self actuation at the A_s temperature. The present work focuses on the processing of a composite solder with nominally equiatomic NiTi particles dispersed in a tin-silver-copper (SnAgCu) lead-free solder matrix.

THIS PAGE INTENTIONALLY LEFT BLANK

II. BACKGROUND

A. SOLDERS IN ELECTRONICS

Lead-containing solder balls have been widely employed in the microelectronics industry for years. However, current industry emphasis is to switch to lead-free solder because of environmental concerns. In Japan and the European Union, lead-free solders have been mandated to largely replace the lead-bearing solders by 2005, with the US microelectronic industry being expected to soon follow the same strict guidelines. As a consequence, a comprehensive understanding of lead-free solders properties and performance in an electronic package is needed for their successful applications in electronics industry.

Ideally, these replacement solder materials would be able to adaptively respond to externally imposed thermo-mechanical deformation to reduce internal inelastic strain concentrations which occur within a joint [2]. Silvain et al. [5,6] has attempted this by incorporating NiTi shape-memory alloy (SMA) particles inside solder. However, they tried to take advantage of the materials superelastic effect, wherein the SMA particles are in the austenitic form and are very stiff. As a result, they could not deform concurrently with the soft solder joints, thus preventing any dividends to be obtained during TMC.

1. Basics

Solder has been used as the most common method of electrical connectivity between silicon chip and printed circuit board structure. Today's package architectures require that solders not only provide the mechanical connection between electrical connection pad and silicon chips, but also provide a means for heat dissipation and structural support during system operation. Being the softest material in the structure, solder plays a vital role

in providing system integrity as well as necessary circuit connectivity in today's microelectronic packaging industry.

The reliability of solders is generally believed to be directly related to their creep resistance and thermo-mechanical fatigue properties as microelectronic solder joints are typically exposed to aggressive thermo-mechanical cycling and creep during service [2]. Improving service performance via microstructural tailoring has continued to be a focus of much research, one of the more promising approaches being the incorporation of compatible reinforcements into a composite solder [7]. However, the thermo-mechanical behavior of many of the proposed lead-free solder composites have not been well understood.

To meet the stringent reliability demands of future microelectronics, a critical assessment of the mechanical, creep and fatigue properties of actual solder balls is required to provide valuable operational specifications for design. The reliability is generally believed to be directly related to their creep resistance, creep-fatigue interaction and thermomechanical fatigue strength.

2. Thermomechanical Behavior

Electronic component packaging, consisting of the electronic device along with its substrate (polymers), undergo an intense range of thermal cycling during normal operation. Operational temperatures of solder joint components range from ambient to 150°C, which is about 0.6-0.8 times the melting temperature of the solder itself. Therefore the solder joints are operated under the regime of high homologous temperature, where homologous temperature is defined as the ratio of the operating temperature and its melting point [17]. As a result, solder joint life is dictated by creep strain range and strain-enhanced coarsening. The effects of these strains and their effects have been widely studied for tin-lead solders such that predictions could be made for joint life [8-16].

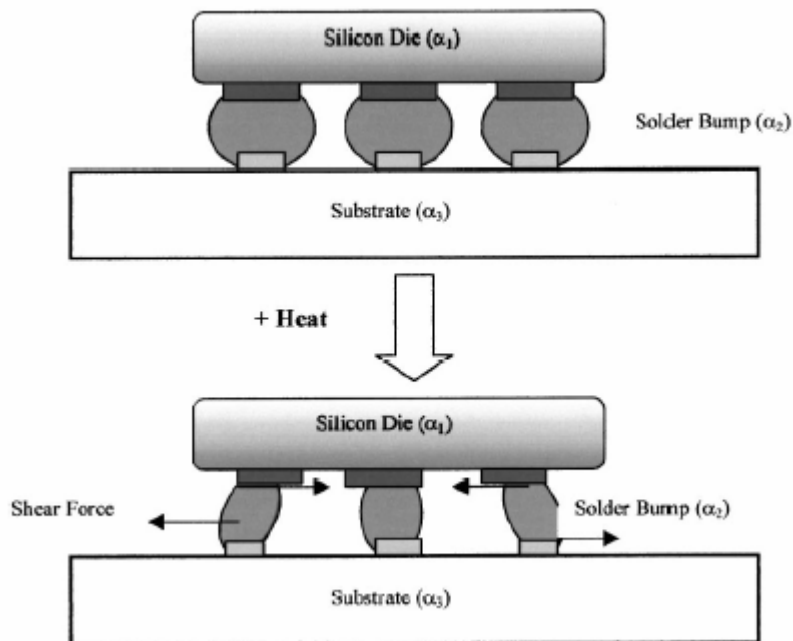


Figure 2. Thermally induced stress that solders may undergo during normal operation [18].

In addition, the thermal expansion of the components under elevated temperatures is another major contributor to the stress and strain in solders during operation. If all the components with the structure have identical CTE and the heat was transferred instantaneously, the effects of expansion and contraction could be ignored. Table 1 illustrates the wide range of CTE values of many components within an electronic package. The CTE of these materials vary by factors as great as 40 times in magnitude, therefore inducing stress and strains that must be considered in the determination of the proper solder alloy. These stresses and strains can possibly promote the crack initiation and propagation in the solder, which lead to the eventual failure of the joint.

Material	CTE ($10^{-6}/K$)	Reference:
FR-4 (PCB material)	11-15	
Epoxies	60-80	
Si	2.6	
Sn-37Pb	21	[21]
Sn-3.5 Ag	22	[19]
Bi-42Sn	15	[19]
Sn-20In-2.8Ag	28.0 at 20°C	[20]

Table 1. CTE data for various components in Electronic packaging [19-21].

Also operationally generated heat, by the joined components, requires dissipation for reliable long-term system operation. Methods for heat dissipation vary widely from heat sinks to external cooling fans varying widely among the different PCB components. Solder joints have also evolved into a major thermal medium during the micro-miniaturization of electronic components. A direct reflection of this occurs in high interconnect BGA devices where some solder balls are placed within the array to provide only as a means of heat dissipation for the component.

With this in consideration, the thermal conductivity of the electronic solder becomes a design aspect of the PCB system. Solder composition can cause a variation in the thermal conductivity and solders must be designed accordingly to ensure the reliability of the joined component. Table 2 gives the thermal conductivity of several currently used solder alloys.

Solder Composition	Thermal conductivity (W/mK)	Reference
Sn-3.5Ag	33 at 85°C	[19]
	54.3 at 23.9°C(w/o contact resistance)	[20]
	36.2 at 23°C(w/o contact resistance)	[21]
	28.2 at 222.9°C	[21]
	28.6 at 246°C	[21]
	29.2 at 256°C	[21]
Bi-42Sn	21 at 85°C	[19]
Sn-20In-2.8Ag	53.5 at 30°C	[20]

Table 2. Thermal conductivity of various solders compositions [19-21].

The limited knowledge of lead-free solder coupled with more stringent operational requirements has caused a revolution in solder joint development. Thermomechanical and fracture characterizations continue for many alternative solder alloys, but no leading replacement alloy has been found. As components continue to grow in size the operational requirements of the solder will continue to be an area of vast research.

B. LEAD FREE SOLDER

1. Introduction

The major solder used for interconnection in the electronic industry to date is a tin-lead (Sn-Pb) alloy. But recent legislative measures, global marketing and the general toxicity of lead have forced manufactures to look for viable lead-free alternatives for this alloy. Ideally,

a replacement for Sn-Pb solders would have a moderate strength, good ductility, possess an appropriate melting temperature, be cost effective, have similar solderability as currently used solders, and be less toxic to the environment [21,22].

Almost 79 alloys have been proposed for a suitable "Pb-free" solder replacement. There is a large disparity of information available on most of the alloys that makes determination of the candidate materials difficult for the electronic industry. Other manufacturing issues of the proposed alloys include cost, availability and the wetting ability with other components within the electronic device.

The electronic industry is very concerned with the reliability of the alloy, due to the fact that electronic packaging density will increase during the evolution of the alloy. Reliability issues include, but are not limited to, mechanical strength, intermetallic compound formed, fatigue resistance and coefficient of thermal resistance.

2. Composite Alloys

A composite material is defined as a mixture of two or more materials. A well-designed composite has a matrix that completely surrounds its reinforcing inclusion materials, where the two phases act together to produce superior characteristics not attainable by either of the constituent materials alone [23]. Since almost all of the considered lead free alloys are based on a tin (Sn) rich composition with a tin rich matrix and a relatively small volume fraction of second phases, compositing has often been utilized in order to enhance the mechanical properties of these alloys. The improved properties of the composite will depend greatly on the size and shape of the reinforcing constituents.

Typical bulk properties of a composite solder material can be directly affected by the adhesion and morphology of

the particulate reinforcement in the matrix. Reliability of composite solder fabrication requires the stability of a clean metallic state of the surface of the reinforcing particles so that the particulates can be well bonded within the matrix of the resulting composite solder [24]. This bonding of the particulates may also modify the microstructure of the resulting solder matrix resulting in drastic changes in solder properties.

A composite solder may also change the characteristics in such a manner detrimental to one of the functions served by solder in the structure assembly. A composite that stiffens the solder could thereby eliminate the strain absorption that protects the very brittle silicon chips.

A characteristic of the composite solder that may provide better resistance to known fatigue life endurance is the goal of the composite. Solder matrixes reinforced with intermetallic or metallic particles have been reported to have superior mechanical properties compared to those of the eutectic solders [26-32]. These types of increases are the desired effects of any lead free solder alternative.

Several studies have been carried out in order to improve and develop methods of constructing composite solder alloys [5-7,15-19,23-34]. The mechanical dispersion of fine particles has been proven through methods of both introduction to paste material and molten solder [32-34]. These introduced particles have provided various results depending on the interaction of the particulate material with matrix [35].

Hard particulate, Cu_6Sn_5 , reinforced eutectic Sn-Pb composite solders maintain ductility, and the average creep rate at room temperature is reduced by one order of magnitude have been demonstrated by Clough *et al* [25]. The solders fatigue life is directly affected by temperature

changes to which components are exposed, causing induced strains resulting from the previously defined CTE excursions [26].

Iron powder reinforced Sn-Bi composite solders have shown 10% higher tensile strength and up to five times the creep resistance in research McCormack performed [30]. The complex loading of solder connected components can cause several modes of tension, shear or torsion that directly influence the deformation of the solder. A well-dispersed foreign particle can serve as an obstacle or hindrances to crack or grain growth.

Subramanian et al [17] pointed out that the increased hardness of some composite solders, due to particle introduction that forms intermetallic compounds, promoted inhomogeneity of strain distribution due to their non-uniform distribution during fabrication. The homogeneity of solder deformation can directly affect the resistance of the solder to creep and TMC fatigue. Therefore the introduced particles must be carefully chosen to ensure that they are uniformly distributed within the solder.

The development of life expectancy models for solder requires insight and knowledge of failure models and constitutive models for the thermomechanical behavior of solders in general, along with a breath of knowledge about their interaction [33]. Solder joints are complex elements of an electronic package and therefore generate complex electrical, thermal and mechanical failure modes.

C. NICKEL TITANIUM

The first steps toward the discovery of the shape memory effect were taken in the 1930s. Very little progressive development was pursued in the field until the early 1960s when Beuhler and his co-workers at the U.S. Naval Ordnance Laboratory discovered the shape memory effect in an equiatomic alloy of nickel titanium [36]. In the past

decades NiTi shape memory alloys have received considerable interest [35-39] because they combine excellent functional properties (one way effect, superelasticity) with a very good mechanical strength and ductility.

1. Basics

Nickel-titanium is a member of a group of metallic materials that demonstrate the ability to return to some previously defined shape or size after being subjected to a define thermal procedure. This group of materials is often referred to as shape memory alloys. These materials can be plastically deformed at low temperatures then after thermal activation can return to initial shape.

Many alloys contain this shape memory effect ability, but the commercial availability of these alloys is limited. Only those alloys that can recover a large amount of strain (approximately 7-8%) or generate significant force upon transformation are cost effective and therefore pursued commercially. Table 4 lists numerous known shape memory alloys, their compositions and transformation temperature range.

Alloy	Composition	Transformation temperature (°C)
Ag-Cd	44/49 at % Cd	-190 to -50
Cu-Sn	~15 at %Sn	-120 to 30
Cu-Zn	38.5/41.5 wt%Zn	-180 to -10
In-Ti	18/23 at %Ti	60 to 100
Ni-Al	36/38 at %Al	-180 to 100
Ni-Ti	49/51 at % Ni	-50 to 100

Table 3. Alloys with shape memory effect characteristics.

The basis of the nickel-titanium system of alloys is the binary, equiatomic intermetallic compound of Ni-Ti. This compound is extraordinary due to the fact it has a moderate solubility range for excess nickel or titanium and exhibits similar ductility comparable to other metallic alloys. This alloy's solubility allows for the alloying of it with many other elements thereby enhancing the overall mechanical and transformation properties of the created compound. Table 4 gives some of the basic properties of binary Ni-Ti alloys.

Property	Property Value
Melting Temperature ($^{\circ}\text{C}$)	1300
Density (g/cm^3)	6.45
Resistivity ($\text{micromho}/\text{cm}$)	
Austenite	100
Martensite	70
Thermal Conductivity ($\text{W}/\text{m}^{\circ}\text{C}$)	
Austenite	18
Martensite	8.5

Table 4. Properties of binary Ni-Ti alloys

Generally materials can be plastically deformed at a low temperature then upon a thermal change will deform themselves back to the "memorized" shape at the lower temperature often referred to as having free recovery. Free recovery is illustrated when an SMA component is deformed while martensitic, and the only function required of the shape memory is that the component return to its previous

shape (while doing minimal work) upon heating. This functional recovery phenomenon is due to the phase transformation within the material.

The shape memory effect is created by a diffusionless, reversible transformation from a low temperature martensite phase to a high temperature austenitic phase. Much research has clarified the crystallographic structure of both the martensitic and austenitic phases of NiTi. NiTi austenite has a CsCl (B2) structure with a lattice parameter $a=0.3015\text{nm}$, martensite is monoclinic 2H with lattice parameters $a=0.412\text{nm}$, $b=0.2889\text{nm}$, $c=0.4622\text{nm}$ and $\beta=96.8$ [36,37]. The structure of martensite allow for the presence of many twin variants, which can all be converted into one primary variant to produce large plastic deformation.

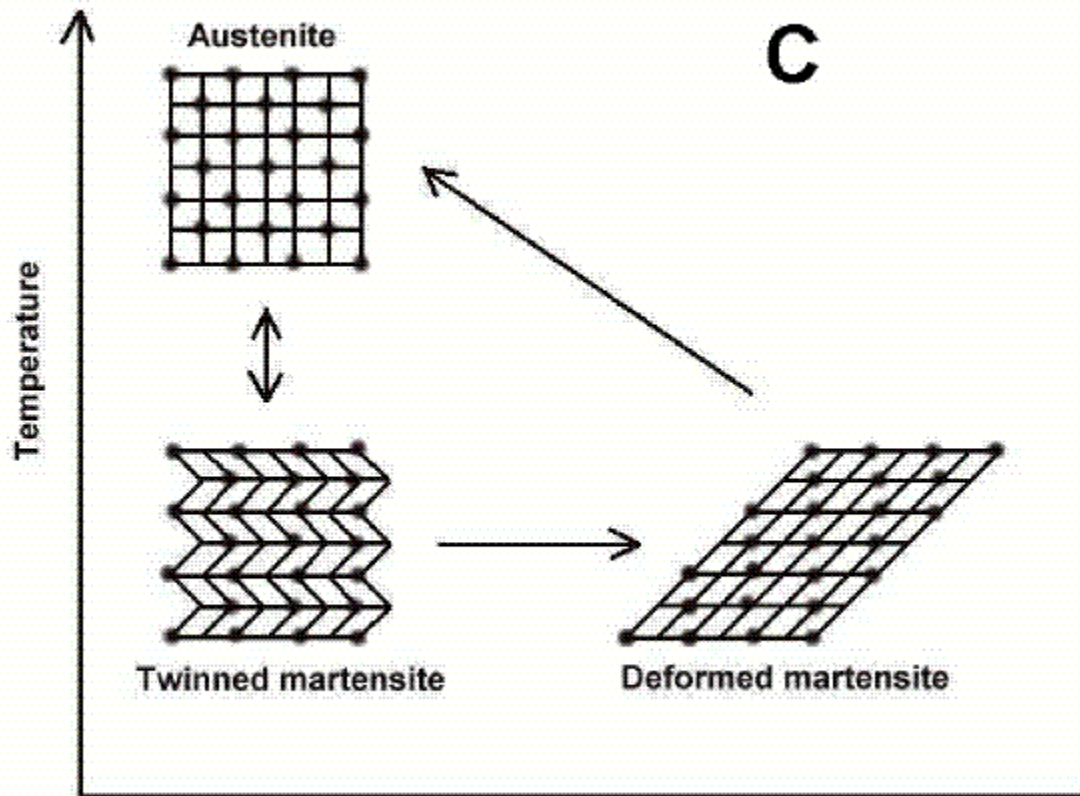


Figure 3. C). Transformation from the austenite to the martensite phase and shape memory effect. The high-temperature austenitic structure undergoes twinning as the temperature is lowered. This twinned structure is called martensite. The martensitic structure is easily deformed by outer stress into a particular shape, and the crystal structure undergoes parallel registry. When heated, the deformed martensite resumes its austenitic form, and the macroscopic shape memory phenomenon is seen [36].

2. Martensite/Austenite Phase Characteristics

The martensite phase of the alloy is characterized by a low energy along with glissile interfaces, which can be

driven by small temperature or stress changes in the alloy. Athermal martensite has a herringbone structure consisting of twin related, self-accommodating variants that cause elimination by other variants during shape change. These self-eliminating variants allow for easy deformation to several percent strain at a low applied stress [36].

The austenite phase of the alloy is characterized by higher energy and upon reaching a determined higher thermal activation will return the structure back to the martensite phase. Also the austenite phase has only one possible orientation, therefore when heated, the deformed martensite phase must revert to the memorized austenite configuration and return to its original shape.

Work hardening or excess amounts of nickel can adversely affect the transformation temperature and yield strength of the phases of the compound. These alterations, which can produce a 50 percent reduction in transformation temperatures in some cases, can change the ease with which the martensite is deformed giving the austenite phase a greater or weaker strength. Therefore the processing of the Ni-Ti alloy is a concern for obtaining proper material characteristics.

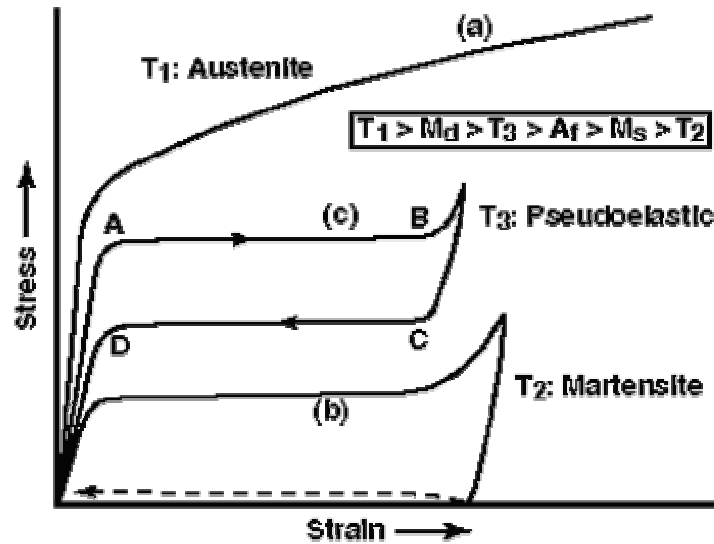


Figure 4. Typical stress-strain curves at different temperature relative to the transformation showing (a) austenite, (b) martensite and pseudoelastic behavior [36].

Operating temperatures of the SMA are very important to the overall characteristic and therefore the transformation range of this alloy. The overall strain that may be recovered during transformation is approximately 8 percent during the normal thermal process. Strains above the limiting value will remain as permanent plastic deformation of the material. These characteristics, coupled with the availability of this material, are basis for selection.

3. Inter-Metallic Wettability

The bond formed between NiTi and most other elements has been documented as poor, due to the reactive nature of titanium, which oxidizes easily. This created wettability problems when attempts are made to bond NiTi to other components via soldering and brazing [5-6,37-39]. Wettability here is defined as the measure of the ability of a material, generally a liquid, to spread over another

material usually a solid [40]. Silvain et al. [6] attempted to overcome this challenge by coating the SMA particles with copper.

Proper wettability requires that specific interactions must occur at the interface between the liquid element and the solid. The wetting term is also often used to describe the ability of the solder to flow over the contact pad area in soldering applications.

The angle between the solid and the liquid provide a measure of the wettability between the two elements as shown in Figure 5. If the angle (θ) lies between 0 and 90° the system wetting is good, whereas if θ is between 90° and 180° , the wetting is considered to be poor.

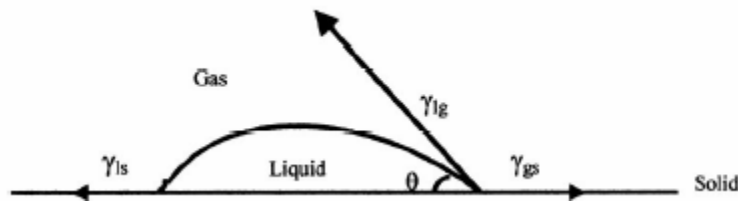


Figure 5. Diagram of wetting angle [35].

The wetting angle is directly affected by many factors such as surface roughness, temperature/time in contact, type of flux used and effectiveness of the flux. Of these factors, studies have shown that more aggressive fluxes are more effective at removing surface oxide layers on NiTi and therefore result in a better interaction between liquid solders and NiTi [39-45]. There are a variety of fluxes available for soldering, depending on the nature of the solder used and the purpose intended for.

It has been contended that Sn-3.5Ag solder paste has a good wettability due in part to the way in which the solder paste is manufactured. A self-fluxed paste would prevent

the formation of oxidation that is detrimental to wettability [43]. Therefore the same idea must be used for the flux selection of the nickel titanium flux selection.

III. EXPERIMENTAL PROCEDURE

In the previous sections, techniques have been reviewed with respect to eligibility for characteristics influencing the suitability for a composite Pb-free solder. The desire for increasing particular properties challenged the development approach in various aspects addressed in this section. The recipe for producing a NiTi-solder composite will be described here.

A. NICKEL TITANIUM SIZING

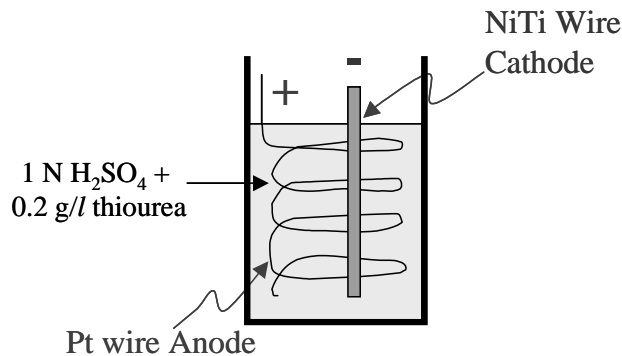
Commercially available 1 millimeter diameter NiTi wires containing approximately 50.6% Ni, and a nominal A_s temperature of 95°C was selected for use in this study. This wire was chosen for its ready availability. Although it is anticipated that ultimately a different composition with a higher A_s temperature will need to be used, the processing route developed here should be independent of the precise composition of the NiTi used. The large size of the wire required the development of a methodology for reducing the wire to approximately 10-20 μm -sized particulate for eventual incorporation into solder.

1. Procedure

Ms. Z. Hang and Dr. B. Majumdar of New Mexico Tech developed the method used in the current study to reduce the wire. The as-received wire was first hydrogen embrittled and then carefully ground to sub-15 μm particles.

The commercial NiTi wire (1mm in diameter) was purchased from Dynalloy Corporation, Costa Mesa, CA, and were first hydrogen (H_2) embrittled and then ground to powders less than 15 microns by mechanical grinding in a mortar and pestle. Before the H_2 embrittlement, the wire was first annealed at 600°C for 2 hours so that it can be rolled into a flat strip with a thickness of approximately 200 μm .

The solution used for H₂ embrittlement of NiTi is comprised of one normal of sulfuric acid and 0.2 grams per liter of Thiourea (Aldrich chemical T33553-500g). In this study, the 1N H₂SO₄ solution was produced using 1 part 95-98% H₂SO₄ (Aldrich chemical 25810-5) diluted by 17 parts of distilled water. A 0.5mm-diameter platinum wire (Aldrich chemical 26722-8) was employed in a coil shape as the anode, and the NiTi wire was used as the cathode in an electrochemical cell, in order to cathodically charge the NiTi with H₂. The oxide layers on the annealed NiTi strip surfaces were carefully removed by grinding with 320-grit silicon-carbide sandpaper prior to embrittlement. A Hewlett Packard power supply has been employed with a capability of 0-10 Volt and 0-1 Ampere for embrittlement. A current density of 35mA/cm² has been adopted to optimize the H₂ evolution rate so that the required of H₂ would diffuse into NiTi. The NiTi strip has been typically embrittled for 4-6 hours in the solution. A schematic of the setup of hydrogen embrittlement is shown in Figure 6.



**Cathodic Charging
with Hydrogen for
Embrittlement**

Figure 6. Hydrogen embrittlement setup.

After the hydrogen embrittlement is completed, the brittle NiTi strip was thoroughly rinsed with distilled

water to remove the residual acid solution from its surface, following by an air dry. The embrittled NiTi strip was subsequently ground in a mortar and pestle for approximately 4-5 hours. The average size of resultant powder has been found to be about $11\mu\text{m}$, as shown in Figure 7.

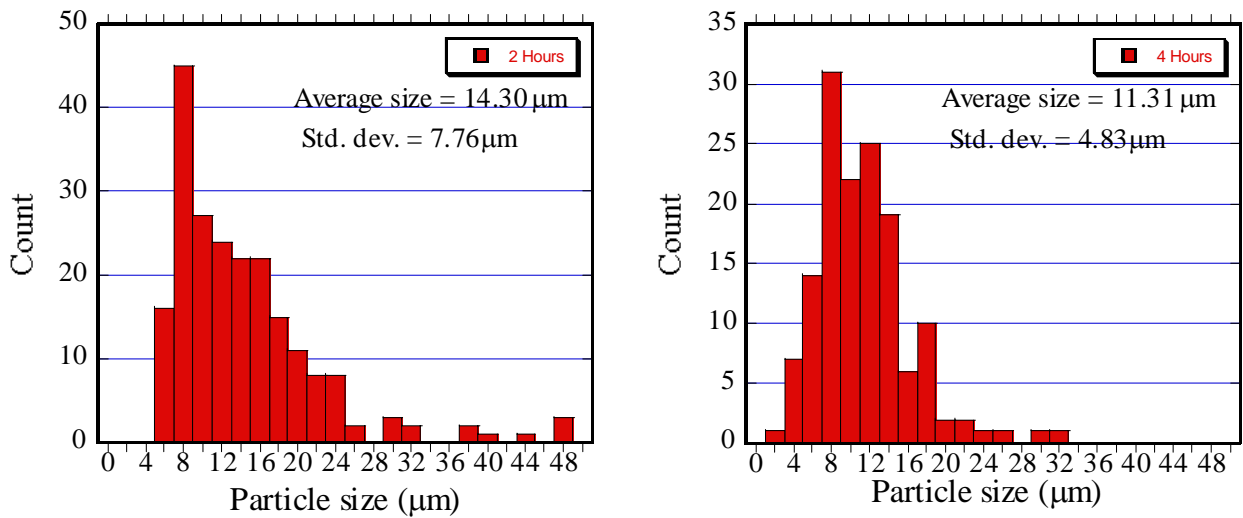


Figure 7. Graphs of particle size distribution for Dynalloy $A_s=45^\circ\text{C}$ wire of 1mm diameter after 2 and 4 hours of mortar and pestle grinding following hydrogenation.

Since a significant amount of cold work has been introduced to the NiTi particles by mechanical grinding, the fine particles have been annealed after grinding at 600°C for 2 hours in order to recover the high dislocation density in the particles.

B. IMPROVING WETTABILITY

As discussed in Section II, the bonding, or wettability, of NiTi with Sn-bearing materials is usually poor due to the inherent oxide layer present on the surface of NiTi particles. Therefore, the oxide layer on the NiTi surface has to be removed before accommodating the NiTi particles into SnAgCu solder [35]. In this study, a hydrofluoric-acid-based flux, i.e. Indalloy™ flux#2 (Indium Corp. of America), has been employed to eradicate the oxides on NiTi surface [45].

1. Procedure

Indalloy flux #2 showed significant wetting improvement during dip tests of NiTi into molten SnAgCu solder. Therefore it was thought that mixing it with the NiTi powder that was previously produced would enhance the composite matrix bonding with the NiTi.

First, the appropriate amount of Indalloy flux #2 was weighed on a Mettler AT 201 scale then added to a plastic beaker. Basing the amount of solution on the 85/15 percent volume ratio of NiTi powder material to flux, recommended by the manufacturer, ensured entire material coverage during mixing. Mechanical mixing of the NiTi powder with a plastic ladle while in the flux ensured particle coverage and insured that the entire batch of powder was successfully deoxidized. The intense stirring of the mixture of powder and flux was continued for approximately 15 minutes.

The material must be used immediately due to the evaporation of the flux. If not used immediately results have shown that remixing the materials provide adequate deoxidizing but required more time to cover all the powder material during mixing. Figure 8 shows the resulting NiTi/flux paste.

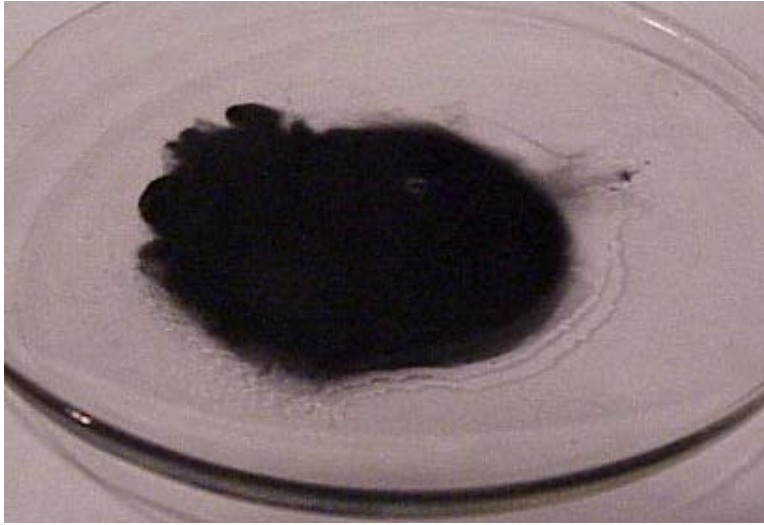


Figure 8. Developed NITI paste.

C. SOLDER FLUX

The next step in the development process is the production of the solder flux. This solder flux is particular to the production of solder bumps used in microelectronics. This flux was developed using a method similar to that developed by Fang et. al [46-48]. The flux uses a low reflow temperature and is self-cleaning. The process that was used to produce the flux is defined below.

1. Procedure

The solder flux is composed of 20 grams of polyethylene glycol (PEG, Aldrich # 20,243-6) a white waxy solid, 15 grams of Adipic acid (Aldrich # A2635-7) a white solid powder and 50 grams of polypropylene glycol (PPG, Aldrich # 20,235-5) a transparent glycerin-like liquid a colorless water-like liquid, the constituents were placed in suitable sized glass laboratory beaker, and the mixture was stirred with a Stir-Pak laboratory mixer Model No. 4554-12 and associated impeller type mixing blade, while being heating with a Thermolyne Model HP-A1915B hot plate, until a temperature of 200°C is reached. The initial stirring speed

is 50 to 100 RPM to provide thorough mixing of all ingredients. The temperature of the solution during stirring was carefully monitored and when the temperature reached approximately 150°C the mixture started smoking. When the mixture reached 200°C, the stirring rate was increased to 200-300 RPM and this speed was maintained until the mixture turned to one single phase with no particulates. Figure 9 illustrates the solution production setup for flux making.

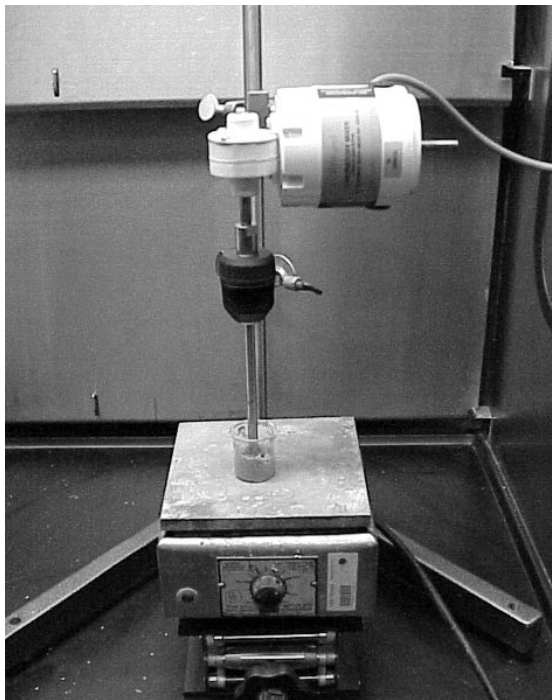


Figure 9. Flux Production Setup.

Once a single-phase solution was achieved, the mixture was removed from the hot plate heating surface and air cooled to approximately 120°C while maintaining the stirring of the mixture at 200 to 300 RPM. The mixing was stopped, the beaker was quickly immersed into a water bath in order to rapidly quench the solution, while simultaneously stirring the mixture at 150 to 300 RPM. This step breaks

down the adipic acid precipitates into fine 25-micron particles (approximate size of SnAgCu powder). Stirring was continued until a solution temperature of 30°C was reached.

At this stage, the solution was transferred to a sealable container (e.g., a suitable lab bottle) and stored at room temperature until ready for use.

D. SOLDER PASTE

The next step in our procedure requires that the solder make the solder paste. In the following, we describe process utilized to make the solder paste [46-48].

1. Procedure

The solder sample batch quantity dictates the amount of flux required to begin the production of the paste. The proper amount of flux to powder determined from the sample batch is based on the weight ratio of solder powder to flux being quantitatively 85% solder powder and 15% flux.

The flux material was weighed with a Mettler AT 201 scale and placed in an appropriate glass laboratory beaker. Now using the determined solder weight, the solder powder was weighed and added to the same laboratory beaker containing the flux. This solution was now thoroughly mixed by hand with a flat spatula, until all the powder particles are covered by flux, producing a gooey consistency.

Once the hand mixing had covered all the powder with flux, the substance was mechanically mixed with the Stir-Pak laboratory mixer and an impeller mixing blade at 200 to 300 RPM. Temperature of the mixture was monitored during mixing, since that this mechanical/chemical process causes an exothermic reaction. This reaction can result in temperature elevation to a range detrimental to the solder during mechanical mixing. The critical temperature that should not be exceeded is 45°C during this step.

Mechanically stirring was continued this mixture until the viscosity of the solution reaches 90 to 100 kila-centa-Poise.

The stirring apparatus was removed and the paste substance placed in an airtight lab container. The paste was stored in a freezer (at least -10°C) until ready for use, except when immediate (less than 2 hours) solder reflow was desired. However the paste was stored in the freezer, prior to reflow and used to form a composite mixture, the paste was allowed to warm to room temperature, in order to use to prevent water contamination from the ambient.

E. COMPOSITE PASTE

Now the development of the composite solder paste will be presented. The previously developed solder paste and NiTi paste were incorporated to make a mixture that ultimately would be dispensed to make the composite solder ball for microscopic observation. The density difference ($\rho_{\text{NiTi}} \sim 6.45 \text{ g/cc}$, $\rho_{\text{SnAgCu}} \sim 7.1 \text{ g/cc}$) between the NiTi and SnAgCu pastes is insignificant and therefore, in principal, it should be possible to produce a uniform distribution of NiTi particles within the solder matrix. The steps used to develop the homogenous mixture of the separate pastes are described here.

1. Procedure

The previously developed solder paste was warmed to room temperature if previously stored in the freezer placed in a laboratory beaker, and mixed with the Stir-Pak laboratory mixer and impeller type mixing blade at 200 to 300 RPM using the same procedure as described in step D. While stirring the paste, the flux-NiTi powder mixture from step B was introduced to the solder paste. The total paste-like mixture was thoroughly stirred until the NiTi powder is evenly dispersed throughout the paste. After about 5 minutes of stirring and the mixture appears homogenous by

visual inspection, mixing was stopped, and the paste prepared for distribution. The reaction occurring within the flux/powder pastes, during deoxidation, is exothermic and the temperature was continuously monitored to prevent exceeding 45°C.

F. PRODUCTION OF COMPOSITE SOLDER

In order to facilitate the characterization of the composite solder sample, the paste was reflowed to a normal solder ball configuration simulating the Ball Grid Array or Flip-Chip balls used in microelectronics. Reflow of the composite solder makes the characterization of the microstructure and physical properties possible. The sample was cross-sectioned allowing determination of the microstructure throughout the entire composite. The cross-section of the solder ball sample then was metallographically polished and inspected in an optical microscope. The detailed description of sample preparation is discussed in the following.

1. Procedure

Approximately 3 cc of composite solder paste, based on knowledge of required solder ball volume, was dispensed from a plastic syringe with an 0.10 mm orifice, onto a 25mm by 25mm aluminum plate substrate which was placed on a hot plate set at 250°C. Approximately 10 seconds after placing the solder paste on the substrate, the composite solder paste began to smoke due to flux evaporation (burn off) and the solder melted. Immediately after melting, the solder coalesced and formed a solder ball. During this process, the flux formed a protective surface layer on the ball, ultimately minimizing oxidation of the solder. Subsequently the flux burned off, as evident by the small air pockets escaping from the molten solder ball. This process is also denoted as the self-cleaning/protective layer process of the solder flux. However using the Indalloy flux #2 for making the NiTi paste was not self cleaning, and this left a slight

blackish residue on the balls after reflow. After a reflow time of approximately 60 seconds, the aluminum plate was removed from the hot plate and air cooled to ambient temperature. The solder ball was then rinsed with methanol to remove all surface contaminants, and ground on one side with 800-grit silicon-carbide sandpaper to reveal the vertical cross-section of the ball, which was then mounted in a metallographic acrylic mount and polished for subsequent microscopic observation. Figure 10 shows an overall view of the resulting composite solder balls produced as described above.



Figure 10. Composite solder balls of ~1mm diameter on an aluminum substrate following surface cleaning.

IV. RESULTS AND DISCUSSION

A. MICROSTRUCTURES

A 1 mm diameter ball sample of monolithic solder was produced by reflowing solder paste only, using the same procedure described earlier for the composite but without the NiTi reinforcement particulates. The sample was mounted and polished, and observed metallographically. Figure 11a and 11b shows the resulting microstructures at 1500X and 3000X, respectively, as observed with a Jenaphot 2000 Optical microscope. As observed here, the microstructure consists of a fine dispersion of Ag_3Sn (and some Cu_6Sn_5) precipitants in a $\beta\text{-Sn}$ matrix. For the small balls reflowed here, very little primary $\beta\text{-Sn}$ is observed in the microstructure.

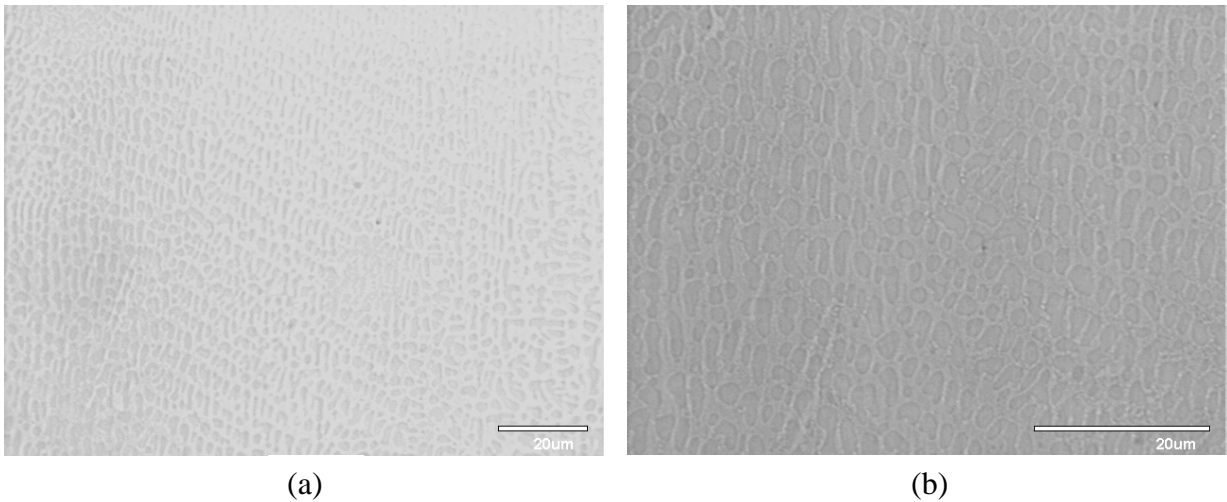
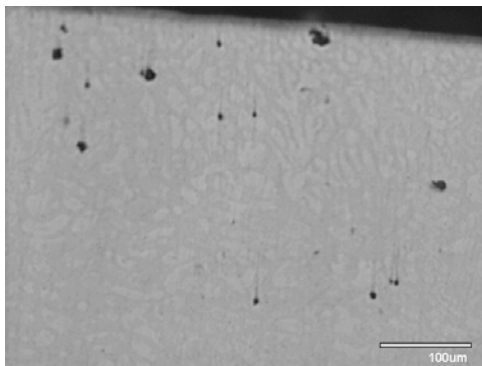
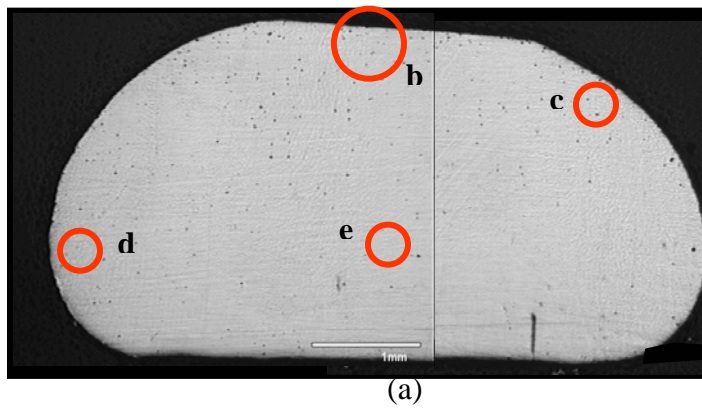


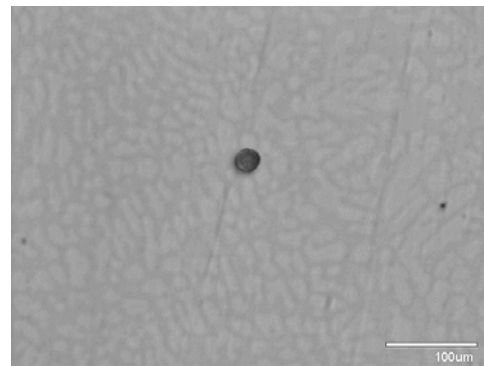
Figure 11. Optical microscopy image of the monolithic solder ball at (a) 1500 and (b) 3000X.

When the same method is utilized to produce a composite of NiTi and solder (i.e. when untreated NiTi particulates are introduced into and mixed with the solder paste), the NiTi particulates were overwhelmingly rejected by the solder melt, as soon as reflow occurred. Since nearly 40% of the paste volume is that of flux, reflow results in a significant volume shrinkage as the solder particles melt and coalesce into a ball near the center of mass, as the flux separates out and forms a protect cover for the ball. Therefore, if the NiTi particles are not wetted by the molten solder, they are not drawn into the melt as the molten solder particles migrate toward the center and coalesce, causing rejection of most of the NiTi particles, which remain near the edges of the ball after reflow.

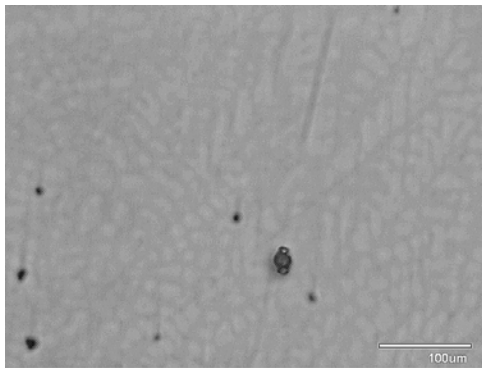
This rejection produces a very low NiTi volume fraction in the ball. Additionally, even when the NiTi particles are incorporated in the melt, they segregate locally, with voids left between the agglomerates due to poor wetting at the NiTi/melt interface. An example of this type of agglomeration with a void is shown in Figure 12.



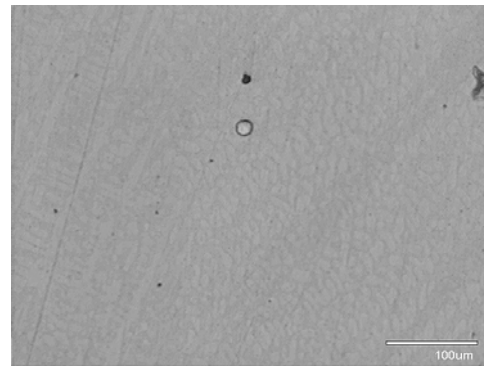
(b)



(c)



(d)



(e)

Figure 12. Microstructure of solder ball with NiTi injected into the melt, showing (a) overall ball and areas of interest, and (b-e) higher magnification pictures showing that most of the NiTi particles are segregated near the top surface.

The initial composite sample agreed with Silvain's previous studies in NiTi, where it was observed to be wetted poorly by solder [5,6]. Also determination of the particle size showed that the NiTi particles needed more grinding to provide a smaller overall size (~11 μ m, i.e., smaller than the solder particle size ~25 μ m), such that the particles were less susceptible to rejection by the moving melt.

In order to circumvent this problem, a different methodology for producing the composite solder was attempted. In this methodology, the NiTi powder was ground for an additional 2 hours and mixed with ~20% PPG. The monolithic solder was then reflowed on an aluminum plate at 250°C, and the mixture of NiTi particulates and PPG was injected into the molten solder ball with the syringe. Following the introduction of the NiTi particles, the solder was solidified. However, this produced a solder ball with few NiTi particles, most of which appeared to segregate near the top surface of the ball. This is shown in Figure 13, which shows the particulate segregation along the edges of the cross-section.

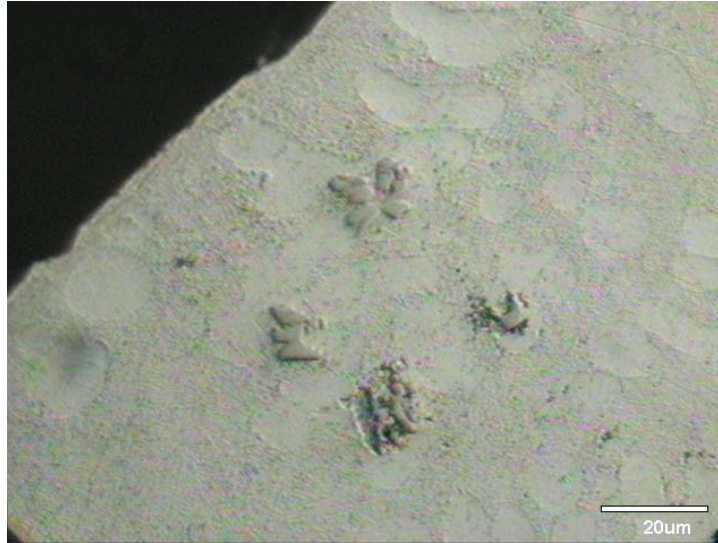


Figure 13. Particulate segregation near surface of ball when injected with PPG.

The final composite methodology was to combine the developed smaller NiTi, and the solder pastes as described in IIIIE. The resulting solder ball showed significant improvements in the particle retention, agglomeration of matrix components, and overall homogeneity of the composite structure as illustrated in Figure 14. The volume percentage of NiTi paste was increased from previous attempts thus providing a distribution not achieved when using the larger sized particles. The smaller NiTi particles permitted ease of containment during the coalacsing of the solder paste to the ball form, therefore more particles remained within the matrix as the ball was formed.

The increased homogeneity was attributed to the smaller particles as well as the increased wetting of the particles by the Indalloy flux. The better formed bonds between the matrix and the introduced particles allowed agglomeration within the melt that eliminated the porosity

seen in previous attempts. Less rejection of the particles provided for a larger volume fraction of particles within the melt, therefore better distribution of particles.

Voids that occurred were at a minimal and some were attributed to particle rip out during the polishing of the surface. NiTi particles did not lump together significantly as noticed in samples, therefore less areas for entrapment of gas bubble (void) formed as the flux was burning off. Small numbers of particle occasionally clumped together but due to the smaller particle size the inclusion area was minimized within the melt such that surface tension of the melt was large enough to overcome pressure formed during the reflow evolution.

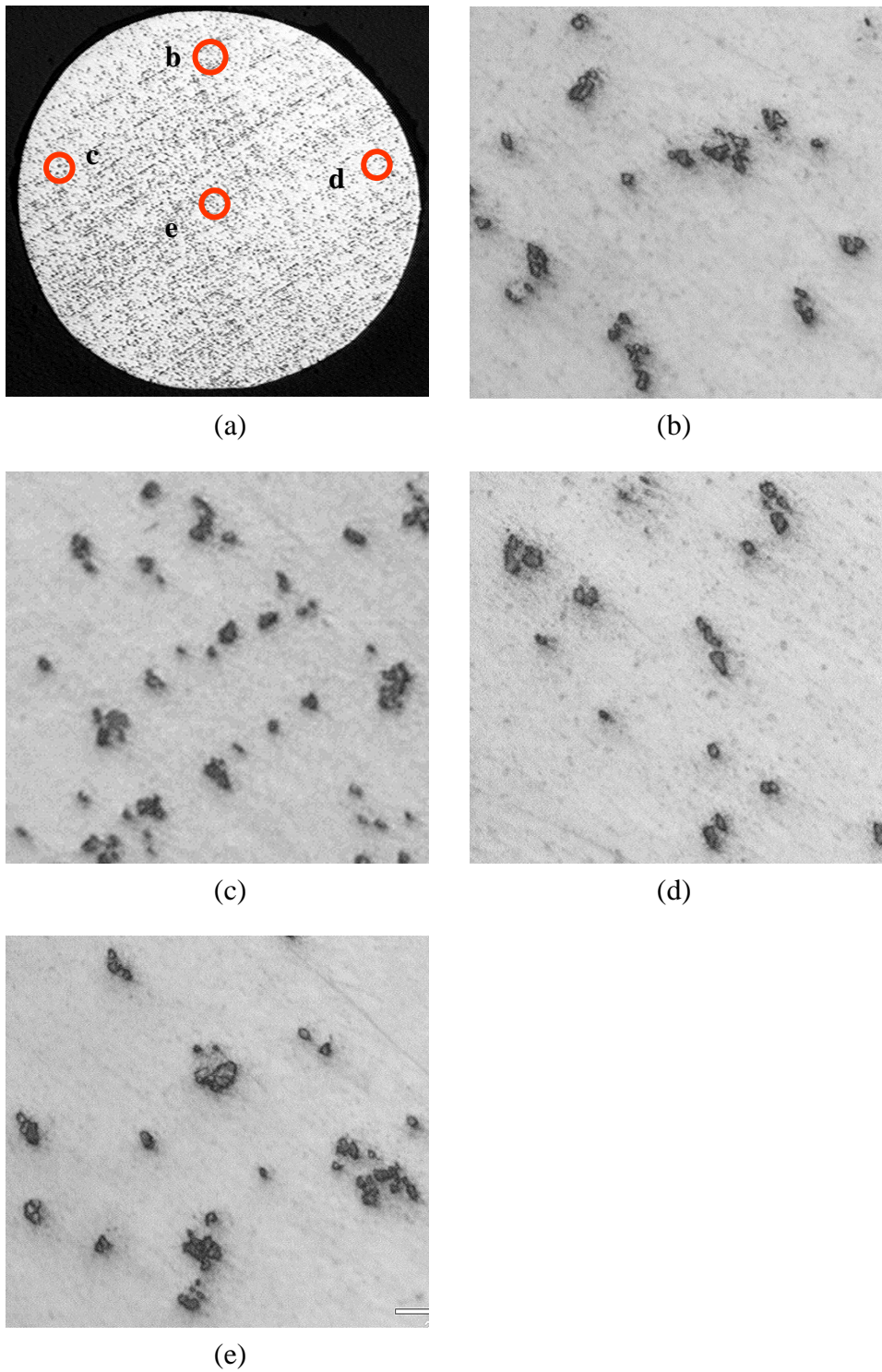


Figure 14. Overall microstructure of the reflowed composite ball produced using the final methodology using a combination of solder paste and NiTi paste (a), along with microstructures of several regions in the ball (b-e), showing a uniform distribution of ~20 volume percent NiTi particles in SnAgCu.

B. INTERFACIAL CHARACTERIZATION

Optical microscopy techniques were initially utilized to evaluate the particle matrix interaction. At the interface, the NiTi appears to form a very small reaction zone with Sn, consistent with later documented analysis. But the introduction of the NiTi reinforcing phase of material did not cause the formation of voids (porosity) in the composite solder microstructure as in previous attempts. Figure 15 gives a 3000X optical representation of NiTi particulate within the composite matrix.

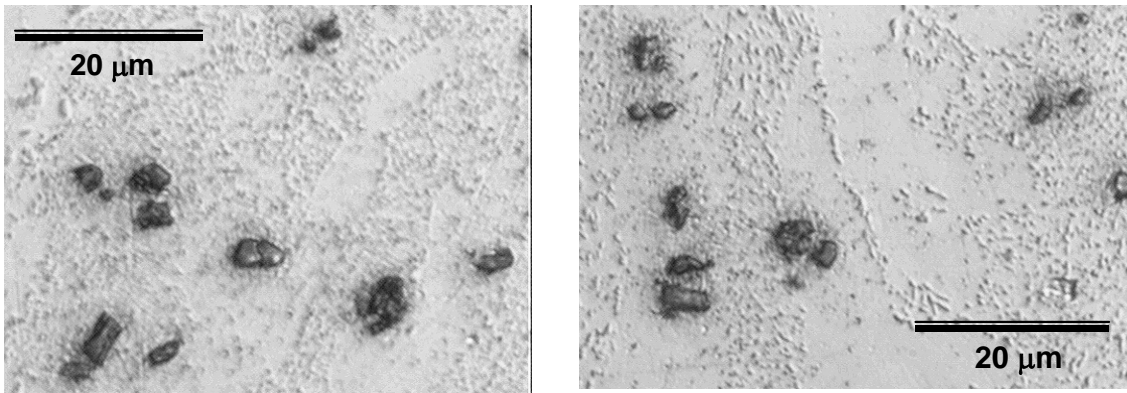


Figure 15. Resulting NiTi solder interfacial zone using 3000X optical microscopy.

The Topcon 510 Secondary Electron Microscope was used in a EDX (energy dispersive X-ray) line scan of NiTi-matrix interface to determine the nature of the interface, and verify whether a significant amount of NiTi has reacted with the molten solder during the 2 minute reflow. A typical line scan of the NiTi/matrix interface zone is provided in Figure 16.

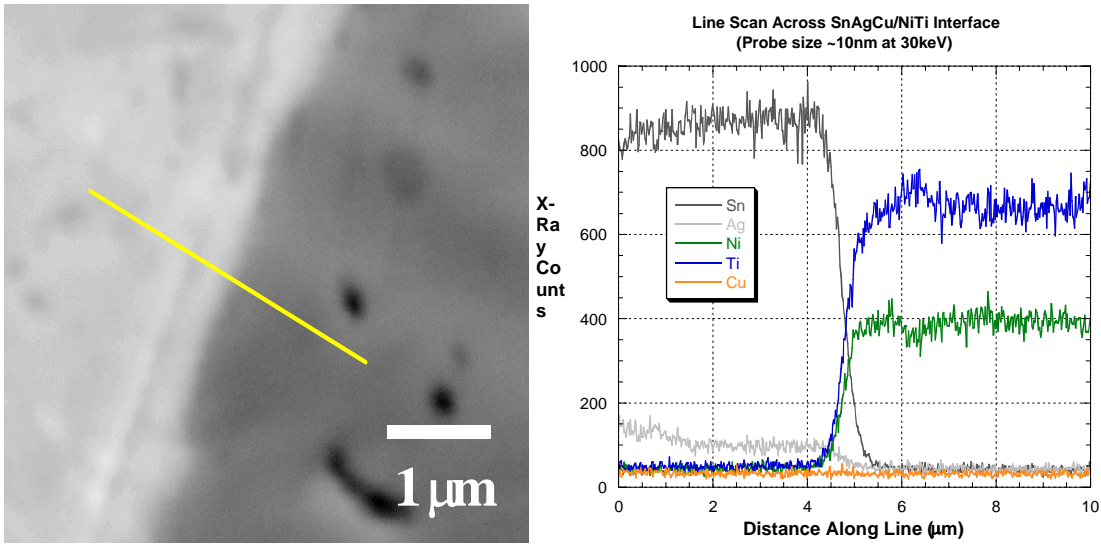
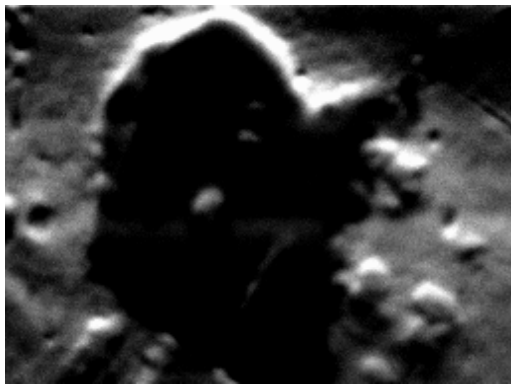


Figure 16. Image and line scan of NiTi/solder interface.

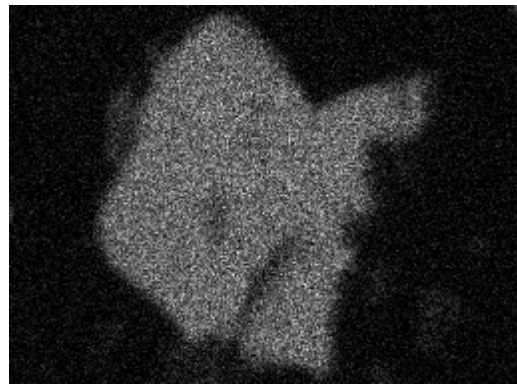
Figure 16 shows a secondary electron (SE) image of NiTi/solder interface and X-ray intensities corresponding to the line scan across the interface shown in the SE image. A small interfacial interaction is noted and although it appears to be $\sim 1.5 \mu\text{m}$, in actuality, this is expected to be even narrower, since electron beam spreading in the X-ray interaction zone is expected to widen the appearance of the interfacial zone in the X-ray line scan. Importantly, no clear evidence of intermetallic formation (either Ni-Sn or Ti-Sn) at the interface is observed, even though a slight inter-diffusion zone is evident.

The Topcon 510 Secondary Electron Microscope also allowed for the analysis of particulate morphology, size and conglomerate formation within the matrix. As noted previously images illustrating the interfacial interaction between the matrix and particles seemed sufficient for good composite formation. Elemental X-ray mapping of the immediate vicinity of a particular NiTi particle within the solder matrix provided confirmation that the NiTi particle retained its elemental composition without extensive reaction with the surrounding Sn. This is shown in Figure

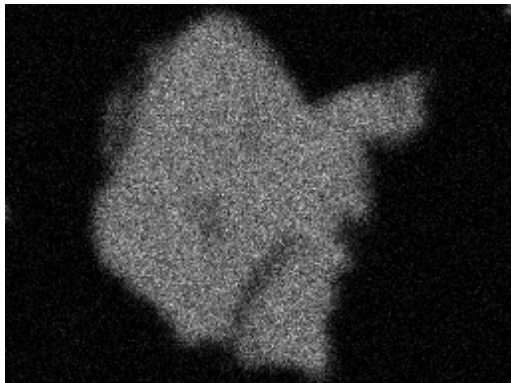
16a-e. Around the NiTi particle, many Ag₃Sn dispersions are observed as evident by the Ag segregations noted in Figure 16d. It can also be seen from the image that the grinding of the NiTi powder resulted in cracking of the reinforcing particle, illustrating the sensitivity of elements and therefore the composite structure to the processing methods as previously observed.



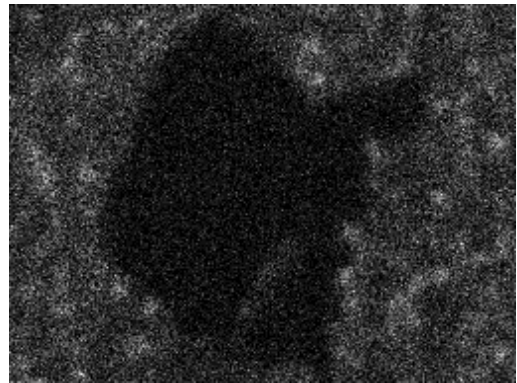
(a)



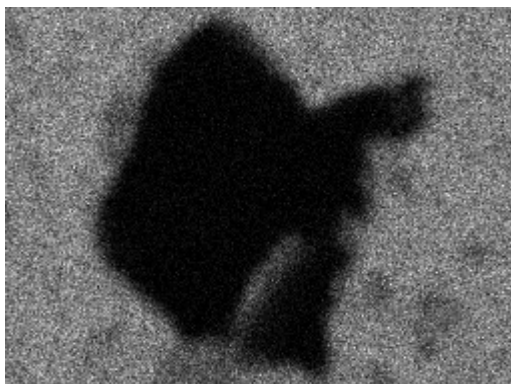
(b)



(c)



(d)



(e)

Figure 17. SEM image and elemental X-ray maps illustrating (a) BSE image, and maps of (b) Nickel, (c) Titanium, (d) Silver and (e) Tin obtained from a region of the composite solder near the vicinity of a NiTi particle.

THIS PAGE INTENTIONALLY LEFT BLANK

V. SUMMARY

In this study, a solder flux production methodology has been implemented to craft a solder paste with similar reflow characteristics to those used in the electronics industry on PC and BGA assemblies. The solder paste incorporate a self-cleaning flux, which deoxidizes individual solder powder particles present in the paste, as well as the providing a protective cover on the molten solder during reflow.

NiTi powder ($\sim 11\mu\text{m}$) has been successfully produced from commercially available wire, by electrolytic hydrogen charging of a NiTi wire cathode to produce embrittlement, followed by a manual grinding to produce average particle size $\sim 11\mu\text{m}$. The NiTi powder was mixed with a hydrofluoric acid based commercial flux in order to form a precursor paste to be used in conjunction with solder paste to form a composite solder. This step allowed deoxidation of the surface of NiTi, thereby activating it for eventual combination with solder.

Separate NiTi and solder pastes were mixed together in appropriate volumetric ratio. The solder paste and NiTi paste were mechanically mixed, such that when reflowed, a typical microelectronic solder ball was produced.

Investigation of the cross-section of the resultant solder ball has shown a homogenous distribution of NiTi particles in the solder ball. Little NiTi particle rejection has been found during reflow. Therefore, the final volume fraction of NiTi retained in the solder ball was consistent with particle introduction during fabrication.

THIS PAGE INTENTIONALLY LEFT BLANK

LIST OF REFERENCES

1. The International Technology Roadmap for Semiconductors, Semiconductor Industry Association, San Jose, CA, 1999.
2. I. Dutta, A. Gopinath and C. Marshall, J. Electronic Mater. 31, 2002, 253.
3. J. H Lau, T. Kruleitch, W. Schar, M. Heyydigner, S. Erasmus and J Gleason, Circuit World, 19, 1993, 18
4. C.P. Wong, J.M. Segelken, and C. N. Robison in Chip on Board technologies for multi-chip modules, ed J.H. Lau, Van Nostrand Rienhold, 1994, pp. 470-503.
5. S. Trombert, J. Chazelas, M. Lahaye, and J.F. Silvain, Compos. Interfaces 5, 1998, 479.
6. J. F. Silvain, J. Chazelas, M. Lahaye and S. Trombert, Mater. Sci. Eng. A273-275, 1999, 818.
7. K. N. Subramanian, T. R. Bieler and J.P Lucus, J. Electronic Mater. 28, 1999, 1176.
8. K. L. Murty, ASME, 1, 1997, pp.1221-1223.
9. W. Yang, R.W. Messler, and L. E. Felton, J. Electron. Mater. 765 (1994).
10. S. Jin and M. McCormack, J. Electron. Mater. 23, 735 (1994).
11. M. L. Huang, C. M. L. Wu, J. K. L. Lai and Y.C. Chan, J. Electron. Mater. 29, 1021 (2000).
12. P. Hacke, A. F. Sprecher and H. Conrad, J. Electron. Packaging 115,153 (1993).
13. D. Frear, S. Burchett, M. Neisen and J. Stephens, Solder Surf. Mt. Technol. 25, 39 (1997).
14. P. T. Vianco, S. N. Burchett, M. K. Neilson, J. A. Rejent and D. R. Frear, J. Electron. Mater. 28, 1290 (1999).
15. P. L. Hacke, Y. Fahmy and H. Conrad, J. Electron. Mater. 27, 941 (1998).
16. V. Sarihan, Journal of Electronic Packaging, 115, 1993, 16.

17. F. Guo and K. N. Subramanian, *Advanced Materials & Processes*, 2002, pp. 10-12
18. J. Van Humbeeck, *J. Mater. Sci. Eng.* 1999; A273-A275: 134.
19. Lee, N. C., Slattery, J., Sovinsky, J., Artaki, I., and Vianco, P., A novel lead-free solder replacement, *Circuits Assembly* 6(10)(1995) 36-44.
20. J. R. Loyd, C. Zhang, L. H. Tan, D. Shangguan, A. Achari, Measurements of thermal conductivity and specific heat of lead-free solder, in: *Proceedings of the IEEE/CMPT International Symposium on Electronic Manufacturing Technology*, Omiya, Japan, 1995, pp. 252-262.
21. H. Walter, Eauserwald, A. Schubert, R. Dudek, B. Michel, reliability evaluations of lead free solder packages.
22. J. A. Jacobs and T.F. Kilduff, in *Engineering Materials Technology*, Prentice-Hall, Inc., Englewood Cliffs, New Jersey, 1976, pp.346-249.
23. J. Sigelo, S. Choi, K.N. Subramanian and J.P. Lucas, *J. Electron. Mater.* 29 (2000) 1307.
24. J. Glazer, *Int. Mater. Rev.* 40 (1993) 13.
25. B. Iring, *Welding J.* Oct 54 (1991).
26. J. L. Marshall and J Calderon, *Soldering SMT*. No. 26, 23 (1997).
27. P. L. Geckle, *IEEE Trans. Comp. Hybrids Manuf. Technol.* 14, 691 (1991).
28. H. S. Betrabet and S. M. McGee, *Scripta Metall. Mater.* 25, 2323 (1991).
29. D. Deborab and L. Chung. U.S. Patent 5089356 (1992).
30. S. Jin and M. McCormack, *J. Electron. Mater.* 23, 756 (1994).
31. C.M. Miller et al., *J. Electron. Mater.* 23, 595 (1994).
32. ASM International, *Electronic Materials Handbook*, Vol.1, Packaging, Materials Park, OH, 1989, p.58.

33. H. Walter, Eauserwald, A. Schubert, R. Dudek, B. Michel, Reliability evaluations of lead free solder packages, Elec. Comp. And Tech. Conf. 2002, IEEE 2002, p. 1246-1255.
34. Guo, F., Choi, S., Lucas, J.P., and Subramaniam, K.N., Soldering and Surface Mount Technology, Vol. 13, no 1, 2001, p. 7-18.
35. E. Hrnbogen In: Bunk WGJ, editor. Advanced structural and functional materials. Heidelberg: Springer-Verlag; 1991:133-163.
36. T. Saburi in: Otsuka k., Wayman CM, editors. Shape memory materials. Cambridge: Cambridge University press, 1998: 49-96.
37. J. Van Humbeeck, J. Mater. Sci. Eng. 1999; A273-A275: 134.
38. T. Duerig, A. Pelton, D Stockel, Mater. Sci. Eng. 1999; A273-A275; 149.
39. Beuhler, Biocompatibility Evaluation of Nickel-Titanium Shape Memory Alloys, 1994.
40. Peter C. Hall, 'Methods of Promoting Solder Wetting on Nitinol', Edison Welding Onst., 125-130, 1997.
41. K. Otsuka, T. Sawanura and K. Shimizu, Physica Status Solidi 5, 457 (1971).
42. K.J.R. Wassink, M. M. F. Verguld, Manufacturing techniques for Surface Mounted Assemblies, Electrochemical Publications Ltd., 1995, GB-Port Erin, British Isle, p.17.
43. M. Abteu and G. Selvaury, Mater. Science and Eng., 27, (2000), pp. 95-141.
44. F. Guo, S Choi, J.P. Lucas and K.N. Subramanian, J. Electron. Mater. 29, (2000), 1241-1243.
45. E. Bastow, Indalloy Corporation internal report.
46. Fang, T., Wiley Encyclopedia of Electrical and Electronic Engineering, Vol. &, 128.
47. Fang, T., Conductive paste, Li, L. and Fang, T.. U.S. Patent 6,451,127, 17 September 2002.
48. Private communications between Dr. Treliaht Fang and Prof. I. Dutta, July 2002.

THIS PAGE INTENTIONALLY LEFT BLANK

INITIAL DISTRIBUTION LIST

1. Defense Technical Information Center
Ft. Belvoir, Virginia
2. Dudley Knox Library
Naval Postgraduate School
Monterey, California
3. Professor Indranath Dutta
Naval Postgraduate School
Department of Mechanical & Astronautical Engineering
Monterey, California
4. Distinguished Professor Anthony J. Healey
Chairman, Department of Mechanical & Astronautical
Engineering
Naval Postgraduate School
Monterey, California